



Nordlaguna – A unique lake basin at the foot of the Beerenberg volcano, Jan Mayen, containing partially enigmatic sediments

Svante Björck^{a,*}, Malin E. Kylander^b, Eiliv Larsen^c, Astrid Lyså^c, Marianne Christoffersen^c, Martin Ludvigsen^d, Stefan Wastegård^e

^a Department of Geology, Lund University, Sölvegatan 12, SE-223 62, Lund, Sweden

^b Department of Geological Sciences, Stockholm University, SE-106 91, Stockholm, Sweden

^c Geological Survey of Norway, Leiv Eriksensvej 39, 7040, Trondheim, Norway

^d Department of Marine Technology, Norwegian University of Science and Technology, Trondheim, Norway

^e Department of Physical Geography, Stockholm University, SE-106 91, Stockholm, Sweden

ARTICLE INFO

Keywords:

Jan Mayen
Volcano
Tephra impact
Land-locked lake
Arctic char
XRF analyses
Clr transformation
Marine-limnic transitions

ABSTRACT

Sediments from the only permanent lake on the island of Jan Mayen (71°N, 08°30'W), Lake Nordlaguna (NL), were investigated. The lake, with an area of ~1 km², is situated at the foot of the world's northernmost active subaerial volcano and is separated from the sea by a 150–240 m wide beach barrier, which reaches 4–5 m above sea level. Most of the lake is deeper than 25 m, with the deepest part being 36 m. Altogether five coring sites, evenly spread out, were chosen and the sediment cores were retrieved from the lake ice with Uwitec and Nesje corers. After detailed descriptions of the very organic-poor and silt dominated sediments (of supposedly tephra-dominated origin), three sites were chosen for further analyses: macrofossils for ¹⁴C dating, tephra chemistry, C, S, grain-size, and XRF analyses. Based on ¹⁴C dates and the occurrence of the so-called Eggøya tephra (AD 1732), age models show variable bottom ages for the three sites: ~3000, 600 and 400 cal yr BP. Due to the position of the core sites, with different sediment source areas, the elemental signals vary considerably between sites. An interesting feature of the lake is an isolated stock of Arctic char, which shows that the now land-locked lake has once been in contact with the sea. The almost total lack of organic material excluded any advanced paleoecologic investigations of the lake, and the study therefore focused on its marine-limnic history by different examinations of the XRF data with focus on the oldest and longest record. This development is based on elemental ratios (Br/Zn), PCA analyses of a center log ratio (clr) transformation of the original XRF data and magnetic susceptibility. It shows that the lake was isolated just before the time of the Eggøya tephra fall-out (~220 cal yr BP), when the stock of Arctic char was most likely isolated from the sea. This was preceded by a ~2200 yr long period of marine bay with a more or less open connection with the sea, and thus varying freshwater impact. Between ~2400 and 2600 cal yr BP the basin was more or less isolated, preceded by almost full marine conditions for at least the 300–400 preceding years we have data from, a period when relative sea level might have been higher.

1. Introduction

The island of Jan Mayen is situated 500 km east of Greenland at 71°N, 08°30'W (Fig. 1A), with a length of 54 km and a width that varies between 2.5 and 15.8 km, and with a total area of 373 km². Jan Mayen is located between the cold East Greenland and Jan Mayen currents in the west and north, respectively, and the warm North Atlantic Current in the east and south (Fig. 1A). This makes it very sensitive to climatic impacts from both latitudinal and longitudinal shifts of these currents, as well as

for changes in the on-going global warming, especially considering the amplified response of the Arctic to this warming. According to personnel at the Jan Mayen Station, sea ice has not been observed around the island since the late 1990s. This accords well with the observed decreasing sea ice extent in the Fram Strait and the Barents Sea since the late 1970s (MOSJ Home page 2019; Polyak et al., 2010), and contrasts with conditions before, and especially during, the Little Ice Age. A high-resolution paleoclimate archive from such a geographically strategic position would thus be of great value.

* Corresponding author.

E-mail address: svante.bjorck@geol.lu.se (S. Björck).

<https://doi.org/10.1016/j.qsa.2022.100060>

Received 28 June 2022; Received in revised form 12 August 2022; Accepted 22 August 2022

Available online 5 September 2022

2666-0334/© 2022 The Authors. Published by Elsevier Ltd. This is an open access article under the CC BY-NC-ND license (<http://creativecommons.org/licenses/by-nc-nd/4.0/>).

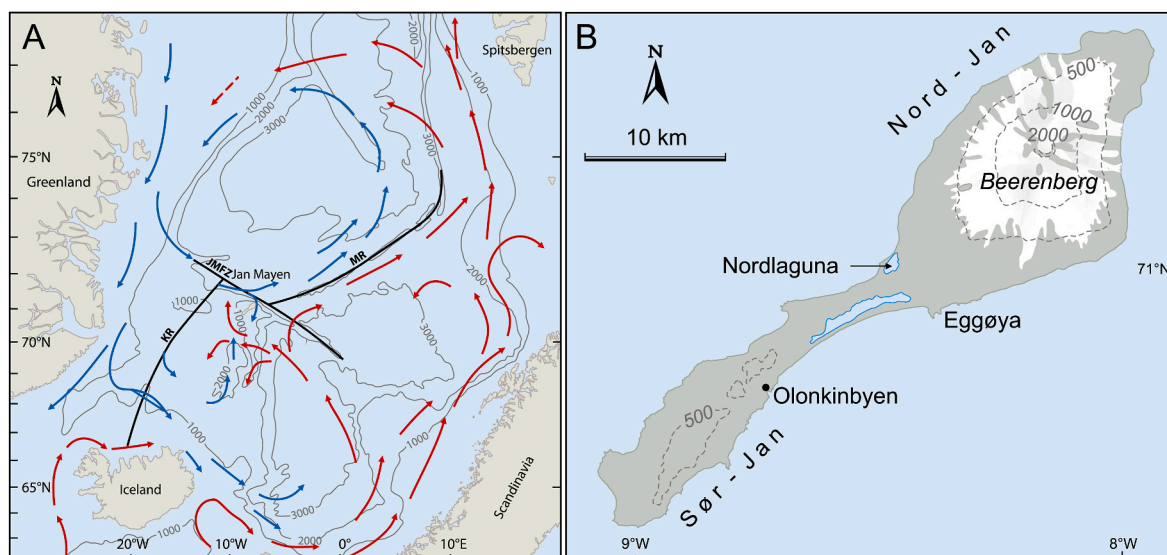


Fig. 1. A. Map of the position of Jan Mayen in the NE Atlantic, showing warm (red) and cold (blue) ocean currents, B. Map of Jan Mayen and the position of Lake Nordlaguna. (For interpretation of the references to colour in this figure legend, the reader is referred to the Web version of this article.)

The only likely continuous terrestrial archive on Jan Mayen is Lake Nordlaguna (NL), situated along the northwestern coast in the central narrow part of the island (Figs. 1B–3A), southwest of the Beerenberg glacier-covered volcano (Fig. 3D). The lake is 1.6 km long and almost 900 m at its widest. Most of NL is > 25 m deep with a maximum depth of almost 36 m in its southwestern part (Fig. 2). The lake is generally surrounded by fairly steep slopes, except at a few places where fluvial fans enter the lake (Fig. 3C).

The lake is situated a couple of meters above the mean sea level of the Greenland Sea, where the local semidiurnal tidal range is 1.5 m, and the lake has no outlet to the ocean, but lake water seeps through the 150–240 m wide beach barrier, Bommen, which reaches 4–5 m above sea level. Heavy storms bring driftwood to the barrier and the lake, as well as ocean water to the lake, witnessed by wash-over channels (Fig. 3B) on Bommen, thereby creating slightly saline water in NL with 3.38–3.40 g salt/liter (3.4‰) in the uppermost 25 m of the water column, which is the deepest sample level we have recent data from. However, Skreslet (1969) measured chlorinity and total hardness down to 35 m in the summers of 1963 and 1965 and - translated to salinity - found an increase from 1.8‰ at 20 m to 2.8‰ at 35 m depth. Together with other parameters (e.g. oxygen, temperature and conductivity) Skreslet's (1969) data showed a clearly stratified water column, while his measurements in the summer of 1963 showed no sign of stratification and, based on the conductivity values, a salinity of ~1‰. These different data, incl. the most recent one (3.4‰), imply large interannual and/or seasonal variations of the lake water column, which are most likely the result of weather related conditions. In fact, the higher salinity of today than in the 1960s may be the effect of the disappearance of sea ice around Jan Mayen during the last decades, resulting in a greater impact of salt water during winter storms on the lake. Storm beach ridges, often consisting of boulders, are common on the Bommen barrier. The importance of eolian activity is revealed by wind ripples between the ridges and by the fact that in winter the lake ice is covered by coarse silt-gravel (Fig. 3D), mainly transported from the barrier and areas with sparsely vegetated terrain around the lake. Wind-derived material is thus an important constituent for the lake sediments when lake ice melts in spring. Other very important sources for the lake sediments are the three valleys Wilzcekaldalen, Stasjonsdalen and Tornøedalen, the latter being the most active at present (Fig. 3C). Run-off through these valleys is only temporarily active, especially during spring melt and heavy rainfall. Temporary snow melt channels are also common on the slopes east of NL.

Sampling of plankton in NL during the summer of 1963 (Skreslet and Foged, 1970), at seven different dates and seven different depths (from 0 m to 34.5 m), showed a total dominance of the halophilous diatom species *Diatoma Elongatum* Agardh, implying fresh/brackish water. Together with *Fragilaria construens*, *Melosira granulata* and *Stephanodiscus astraeta*, these were the only obvious autochthonous species found. The remaining ~50 species were regarded as allochthonous, dominated by fresh-water diatoms from the surrounding landscape and a few true marine species, e.g. *Melosira sulcata*, from direct sea water influx. Samples of benthos collected in the summer of 1965 by Skreslet and Foged (1970) showed a very poor fauna and the authors concluded that NL "is a poor body of water, offering its inhabitants, and especially its population of Arctic char, very unfavourable conditions". Thus, an interesting feature of the lake is the presence of Arctic char, *Salvelinus alpinus* L. (Bird, 1935; Bang and Skreslet, 1965; Skreslet, 1973). This anadromous species must have been trapped in the landlocked lake environment some time ago, and according to Larsen et al. (2021) it occurred through volcano-tectonic uplift across a lake – sea passage at c. AD 1730. The implication is that NL was once regularly connected to the sea, through an outlet in the Maria Musch Bay (Fig. 2), in contrast to present day. Therefore, one important aim of the study has been to establish to what degree and for how long the lake was previously connected to the sea, and how its isolation history is manifested in the sediments.

To disentangle the information archived in NL and its sediments, the area around the lake and the lake bottom have been mapped (Fig. 2). Five cores were sampled from the deeper parts of the lake with the objective to present the available and most interesting data from this unusual lake basin in order to understand its environmental history.

2. Setting

Jan Mayen, the northernmost island of the Mid-Atlantic Ridge, hosts the world's northernmost subaerial active volcano, Beerenberg (2277 m a.s.l.) (Fig. 3D). Four eruptions have been observed, AD1732, 1818, 1970 and 1985 (Sylvester, 1975; Gjerløw, 2019), all along the flank of Beerenberg, of which the AD1732 eruption, called the Eggøya eruption, was probably the most spectacular one. However, Imsland (1978) has estimated a total of at least 75 Holocene eruptions, including several in the southern part of the island (Sør-Jan). The island belongs to the Jan Mayen Microcontinent, which was established in the early Paleogene when the Atlantic Ocean was opened-up (Mjelde et al., 2008). Exposed

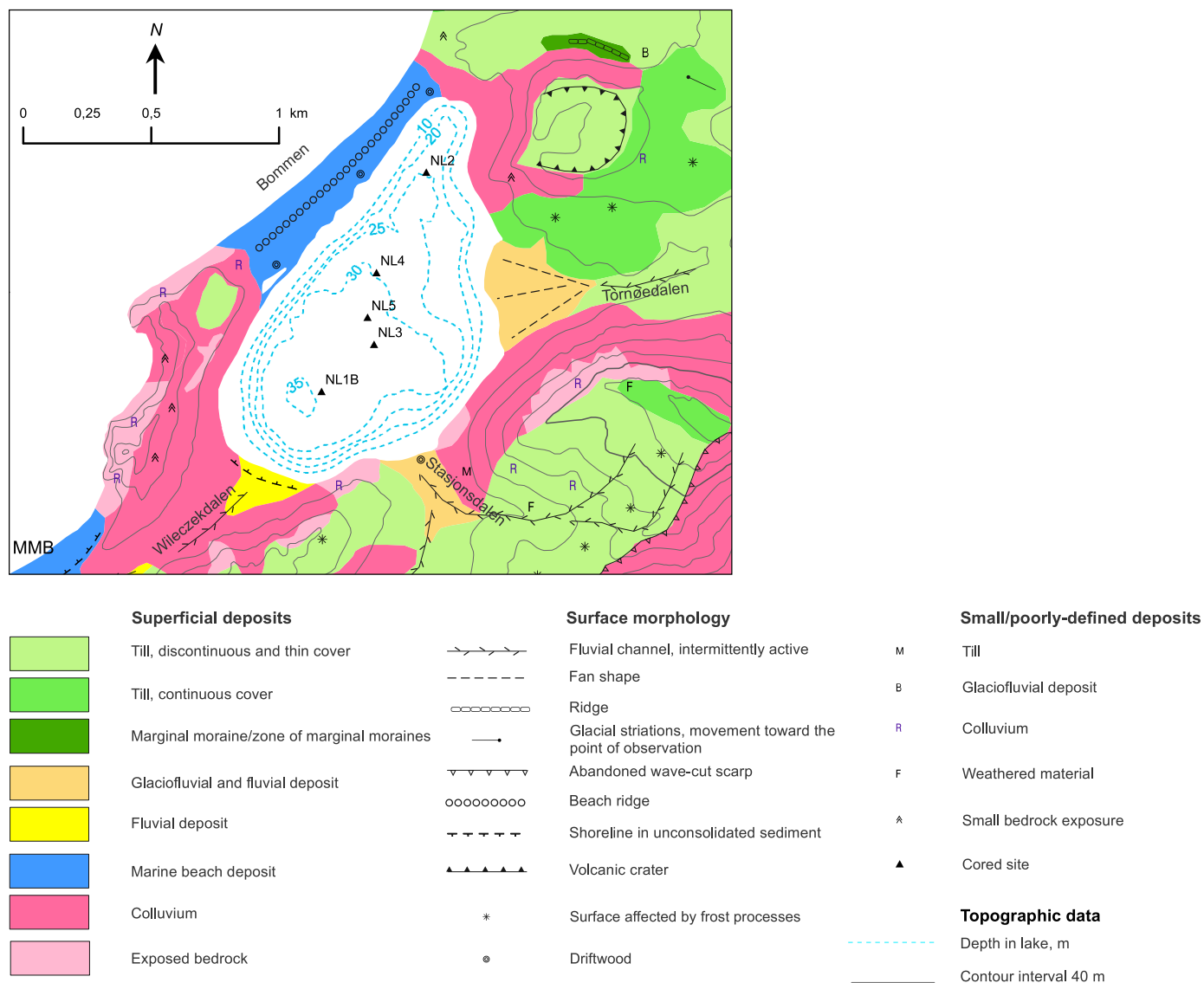


Fig. 2. Geologic and geomorphologic map of the terrain surrounding Lake Nordlaguna from Lyså et al. (2022) (light blue), with the five coring sites marked, and topography marked by 40 m contour lines and lake bathymetry. Note that Maria Musch Bay is marked with MMB in the lower left corner. (For interpretation of the references to colour in this figure legend, the reader is referred to the Web version of this article.)

bedrock on the island has long been known to be of Quaternary age (Fitch et al., 1965; Cromwell et al., 2013). The oldest dated rock from Jan Mayen has now yielded an age of 564 ± 6 ka from a cliff facing NL (Larsen et al., 2021). The entire island, and probably also shallow shelf areas to the south and southeast, was glaciated during the Last Glacial Maximum (LGM) (Lyså et al., 2021). During the Little Ice Age glacier outlets from Beerenberg expanded (Anda et al., 1985) with the potential of increased influx of glaciofluvial material via Tornøedalen to the lake basin. Deposits in the vicinity of the lake are dominated by tills, and by a variety of gravitational slope, beach and fluvial/glaciofluvial sediments (Fig. 2). Resedimented tephra material is an important element of the sediments around the lake and therefore, also within the lake.

The climate on the island is defined as Arctic-marine (Gabrielsen et al., 1997) dominated by strong winds. Average annual temperature at sea level is today close to 1°C , which is higher than during the latter part of the last century when it was below 0°C (Hudson et al., 2019). Since 1921 mean daily temperature for the warmest month (July–September) has varied between 2.5°C (August 1968) and 8°C (September 1934), while the mean daily temperature for the coldest month (January–March) has varied between -14.4°C (February 1943) and -2.3°C

(March 2018). Since 2004 a warming trend is noted, especially in terms of winter temperatures. Mean daily temperatures for the coldest month have not been lower than -5.9°C (March 2011) (<https://www.met.no/vaer-og-klima>). Since 1921 the annual precipitation on the island has varied considerably between 197 and 904 mm, in 1926 and 1972, respectively, often resulting in high humidity and causing the normally foggy weather.

3. Methods and material

Superficial deposits and morphology in and around the lake have been mapped (Fig. 2). Deposits around the lake were documented in the field and georeferenced using GPS, and later processed using ESRI/ArcGIS 10.6 and World Imagery Map Service 2020. The lake bottom was surveyed with a Side-Scanning Sonar (SSS) mounted to an Autonomous Underwater Vehicle (AUV), run in a pre-programmed route covering the entire lake floor. The SSS transmits fan-shaped pulses of acoustic energy along the lake floor to achieve wide vertical images (Klein, 2002). This resulted in an image showing acoustic reflectance of the seabed. A bathymetry model was developed from the ranges measured using the

Table 1

All ^{14}C dates from Lake Nordlaguna (NL). Jan Mayen. Sample depths refer to depth below sediment surface in the four different cores (NL1b, NL2, NL3b and NL4). Cc = whole core catcher, Ccm = middle of core catcher, Ccb = bottom of core catcher. Unid = unidentified to species.

Site name	Sample depth, cm	Material dated	Sample weight (mg C)	^{14}C age yrs BP	Error, 1σ	Lab nr	IntCal20 age range (yr BP), 2σ
NL1b	6 ± 1	Plant macro-fossils, unid	0.5	1165 fM		LuS 12200	End of 1980s
"	7,5 ± 0,5	"	0.6	1021 fM		LuS 12201	Mid 1950s
"	95 ± 1	"	0.3	650	45	LuS 12202	670–553
NL2	27,15 ± 0,65	Plant macro-fossils, unid	0.3	1051 fM		LuS 12203	Mid 1950s or end of 2000s
"	67,3 ± 2,5	Moss and plant remains, unid	0.5	300	35	LuS 12328	463–292
"	80,7 ± 2,5	Moss, leaves, unid plants	0.4	205	50	Lus 12329	422–0
"	94,5 ± 1,5	Moss remains, plant stem, unid	0.2	630	70	Lus 12270	679–524
"	102,5 ± 2,5	Moss, plant and stem remains, unid	0.2	235	55	LuS 12330	453–0
"	106,5 ± 1,5	Plant macro-fossils, unid	0.1	13670	170	LuS 12204	17039–16050
NL3b	Ccb	Plant macro-fossils, unid	0.1	365	70	LuS 13277	520–295
"	Ccm	Mainly mosses with some plant remains	1.1	155	40	LuS 13278	286–0
NL4	83,5 ± 1,5	Plant macro-fossils, unid	0.1	995	200	LuS 13283	1297–563
"	126 ± 2	"	0.1	2220	100	LuS 13282	2489–1940
"	163,75 ± 1,5	Mosses, possibly terrestrial	1.2	2535	40	LuS 13281	2751–2490
"	166,5 ± 1,5	Mosses and a few plant remains, unid	0.3	2850	45	LuS 13280	3145–2850
"	Cc	Mainly mosses	1	3015	40	LuS 13279	3345–3074

vehicle mounted Doppler Velocity Log (DVL). A simplified map is shown in Fig. 2. The SSS data also show driftwood and flooded and washed-in remnants of the American base Atlantic City from the 1954 storm (Christoffersen, 2018), which was situated in the northwestern corner of the lake, at the far left corner of Fig. 3A.

Partly based on the SSS data, five coring sites were selected: NL1–NL5 (Fig. 2). NL1 and 2 were cored in 2016 with a Nesje corer while NL3–5 were cored in 2017 with a Uwitec piston corer, both systems with sampling tubes of 11 cm diameter. NL1 is the deepest site (35.8 m water depth) where two corings (A and B) were performed, of which the first one (A) was disturbed and only 23 cm long. It was, however, opened up in the field to get an idea of the character of the sediments, while NL1B was saved. NL3 and NL5 are situated in ~34 m, NL4 in ~30 m and NL2 in ~25 m deep water. The sediments were extremely hard to core, likely due to the compactness and high friction of deposits dominated by volcanic derived material. NL4 was the longest sequence retrieved, 154 cm, although 25–30 cm was lost from the core top. From the other coring sites, we retrieved 92 cm (NL1B), 98 cm (NL2), 32.5 and 100 cm (NL3A and NL3B) and 55.5 cm (NL5).

All cores were kept in the PVC tubes and stored in the cold room at NGU in Trondheim. There they were first logged for density, magnetic susceptibility and fractional porosity then split into halves where their lithology was described in detail, of which three are presented here (Fig. 4). One half was sub-sampled for discrete analyses while the other half was kept for XRF core scanning and archiving.

Elemental analyzes were carried out on three cores, NL1B, NL2 and NL4, with a high-resolution ITRAX XRF core scanner at the SLAM Laboratory at the Department of Geological Sciences, Stockholm University. Cores were scanned at a resolution of 200–500 μm , with higher-resolutions used on laminated sections, and a Mo tube set at 30 kV and 50 mA with 15 s exposure times. The original data were handled using a center log ratio (clr) transformation on selected elements so that the changes are independent of the closed-sum effect (Weltje and Tjalvingii, 2008).

At the NGU sediment laboratory grain-size analyses were carried out on NL1B, NL2 and NL4 with a Coulter Counter (Suppl. Mat. Table 1). Furthermore, a total of 20 analyses for C and total organic carbon (TOC) were performed on NL1B, NL2 and NL4 and four analyses for S on NL4. The main objective was to support the lithologic descriptions and help establish the sedimentary environment.

Altogether 16 sample levels from four of the cored sites were radiocarbon dated (Table 1). Oxcal (Version 4.4.3) (Bronk Ramsey, 2009) with the IntCal20 Northern Hemisphere calibration curve (Reimer et al., 2020) was used for calibrating all the dates, and all ^{14}C dated samples were pre-treated and measured at the Lund University Radiocarbon Dating Laboratory. All samples consisted of washed and

sieved macrofossils, of which three were samples from the core catcher. In addition, twenty samples were submitted for ^{210}Pb dating, but the activity was too low for reliable measurements.

A total of 10 supposedly primary tephra layers were prepared for electron microprobe analyses using wavelength dispersive spectrometry at the Department of Earth Sciences, Uppsala University, Sweden and the Tephra Analytical Unit at University of Edinburgh, UK. Three samples analyzed in both Uppsala and Edinburgh show good agreement between mean values, but with significantly more spread in the analyses from Uppsala University (Table 2). The 10 analyzed samples are from NL1B, NL2, and NL4.

Eleven test samples were submitted for diatom analyses from NL1B and NL2, but the sediments were generally extremely barren of diatoms, in spite of reports of a fairly varied diatom flora in the lake (Skreslet and Foged 197). However, a few benthic brackish-fresh water diatoms were found in two samples from Unit 3 in NL2 and in one sample of Unit 2 in NL1B.

4. Results and discussion

Since NL4 is the longest core, both length-wise and time-wise, much of our results and discussion will focus on this core. However, we will also include results from NL1B and NL2, from which we have as detailed XRF data as in NL4, to obtain a larger picture of the development of Lake Nordlaguna.

4.1. Lithology

The overall lithology of the five coring sites is summarized in Suppl. Mat. Table 1, and the lithologies of the three discussed cores are depicted in Fig. 4. A common feature of the sediments is their dark colour and compact nature, the large influence of tephra material, the very low organic matter content and the dominance of silt sized particles. Apart from silty units, some are also clayey, while others are richer in sand with occasional gravel. Some units are laminated (varved?) whereas others are disturbed. Boundaries between units can be gradual, inclined, very sharp or erosional, witnessing a dynamic sedimentation environment.

In this context the Eggøya eruption in AD1732 (Gjerløw et al., 2015) is an important marker, not only in terms of lithology but also its impact on the sedimentation and as a time marker. For this reason we have analyzed the geochemistry of 22 suspected tephra samples from the cores and in the surroundings of the lake. We assume that the first (oldest) occurrence of a tephra with the Eggøya signature in the three lake cores is the primary Eggøya tephra, while younger layers with the Eggøya signature are regarded as reworked Eggøya tephra. Accordingly, we have been able to identify the first deposition of the Eggøya tephra at

Table 2

Average major-element compositions of tephras successfully analysed by EPMA presented as oxide weight-percentages (wt%), with 1 sigma standard deviations (sd) and number of successful analyses (n) for each sample.

	Number of analyses (glass)	Mean + 1 sd	Na2O	SiO2	Al2O3	MgO	K2O	CaO	TiO2	P2O5	FeO	MnO	Total	Comment	
<i>Uppsala analyses (2016 & 2017)</i>															
JM NL1B_35.2 cm	6	mean	3.36	47.40	15.76	4.22	3.07	9.06	3.30	0.79	9.85	0.21	97.01	6.43	Eggöya
		Sd	0.17	0.70	0.32	0.23	0.11	0.34	0.09	0.11	0.30	0.04	1.29		
JM NL1B_47.1 cm	5	mean	3.33	46.94	15.69	4.31	2.96	9.27	3.30	0.74	10.06	0.21	96.81	6.28	Eggöya
		Sd	0.13	0.74	0.27	0.09	0.13	0.11	0.08	0.11	0.21	0.04	0.97		
JM NL1B_65.7 cm	6	mean	3.53	47.01	15.72	4.37	3.09	9.02	3.33	0.74	10.11	0.22	97.12	6.62	Eggöya
		Sd	0.21	0.56	0.51	0.31	0.29	0.54	0.20	0.08	0.32	0.06	0.94		
JM NL1B_68 cm	2	mean	3.48	47.26	16.27	4.47	2.93	9.37	3.11	0.72	9.87	0.18	97.63	6.40	Eggöya
		Sd	0.08	0.37	0.52	0.04	0.13	0.09	0.07	0.00	0.21	0.00	0.50		bad slide, most shards under epoxy surface, can be ground again
JM NL1B_70.6 cm	9	mean	3.56	47.17	16.16	4.39	2.90	9.21	3.23	0.69	10.16	0.19	97.66	6.46	Eggöya
		Sd	0.39	1.23	0.68	0.23	0.28	0.41	0.10	0.13	0.68	0.05	1.72		
JM NL2_78.3 cm	10	mean	3.35	46.38	15.82	4.41	3.02	9.12	3.25	0.72	10.27	0.23	96.58	6.37	Eggöya
		Sd	0.23	0.89	0.34	0.37	0.12	0.41	0.11	0.09	0.40	0.07	1.17		
<i>Edinburgh analyses (April 2018)</i>															
JM NL4_70–71 cm	22	mean	3.54	47.63	15.92	4.17	3.10	9.35	3.23	0.69	10.02	0.21	97.87	6.63	Eggöya 1732
		Sd	0.21	0.46	0.38	0.22	0.20	0.31	0.08	0.03	0.30	0.01	0.67		
JM NL4_96–97 cm_TRACHYTE	4	mean	6.59	65.38	19.22	0.01	7.14	0.80	0.26	0.02	0.51	0.01	99.95	13.73	Only trachytic tephra found, interesting mixed layer, many minerals and tephra of different composition
		Sd	0.09	0.74	0.16	0.03	0.64	0.28	0.19	0.01	0.32	0.03	0.72		not Eggöya (?), but similar geochemistry
JM NL4_96–97 cm_TRACHYBASALT	7	mean	3.49	47.50	15.30	4.15	2.99	9.26	3.52	0.69	10.62	0.22	97.74	6.48	
		sd	0.12	1.22	0.55	0.15	0.21	0.71	0.09	0.07	0.96	0.01	0.77		many uncorrelated shards in this sample MIXED layer, minerals and tephra of different composition
JM NL4_132–133 cm_MIXED	20														
<i>Edinburgh analyses (December 2018)</i>															
JM NL1B_70.6 cm	12	Mean	3.56	48.42	15.64	4.23	3.11	9.20	2.92	0.65	10.13	0.18	98.05	6.67	probably Eggöya, some low Ti shards
		Sd	0.16	0.61	0.27	0.17	0.12	0.27	0.44	0.08	0.26	0.05	1.03	0.24	
JM NL2_78.3 cm	10	Mean	3.68	48.03	15.82	4.27	3.03	9.34	2.79	0.70	10.07	0.17	97.86	6.65	probably Eggöya, some low Ti shards
		Sd	0.43	0.73	0.39	0.19	0.18	0.53	0.63	0.12	0.34	0.05	1.28	0.50	
JM NL1B_65.7 cm	13	Mean	3.71	48.29	15.79	4.10	3.20	9.08	3.17	0.70	9.84	0.21	98.08	6.90	probably Eggöya
		Sd	0.16	0.65	0.26	0.30	0.31	0.82	0.11	0.06	0.42	0.01	0.70	0.41	
EGGÖYA 1732 (Gjerløw et al., 2015)	81	Mean	3.53	47.53	16.22	4.27	3.06	9.32	3.24	0.67	10.35	0.22	98.41	6.59	
		Sd	0.11	0.53	0.21	0.15	0.13	0.28	0.05	0.02	0.30	0.01			

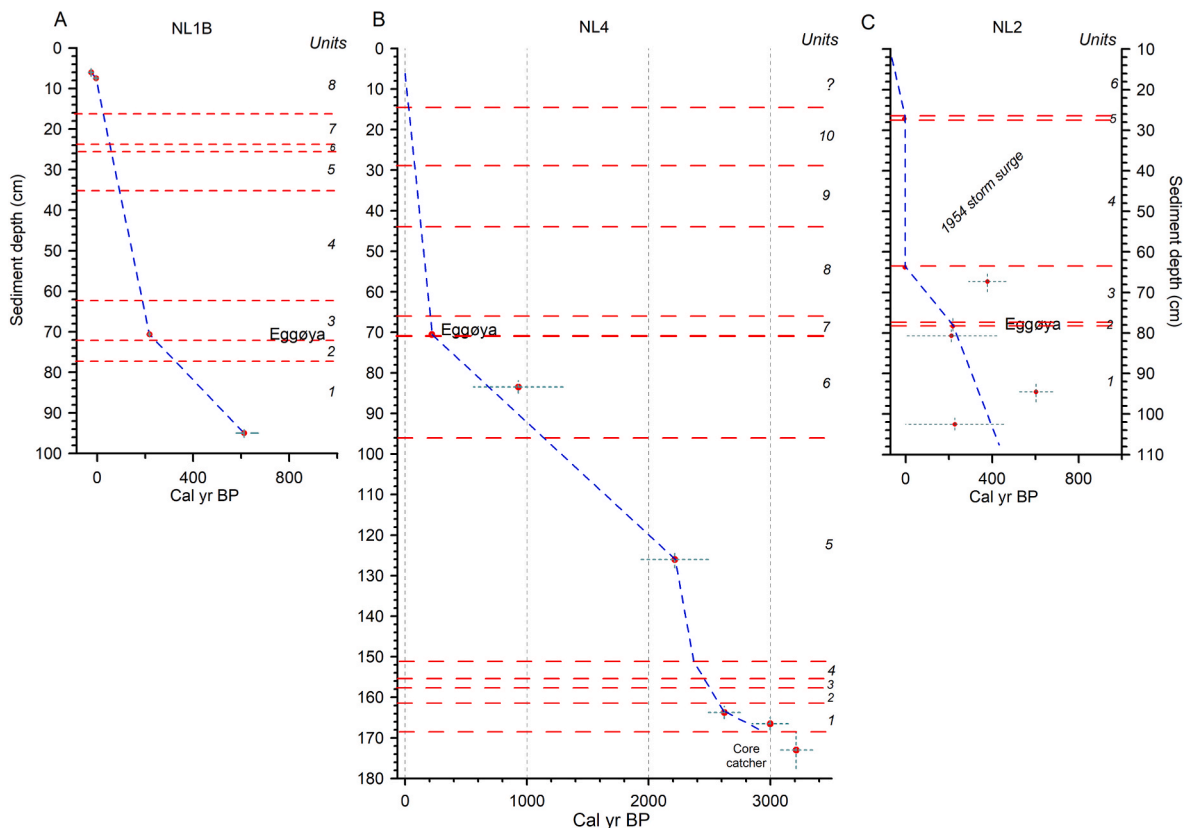


Fig. 5. Age-depth graphs of the three core sites, with the lithologic units marked with red dashed lines and the ^{14}C dates and the Eggøya tephra marked with a red circle, and with a light-green dashed lines marking the ^{14}C dating uncertainty of 2σ . **A.** Age-depth graph of core NL1B. **B.** Age-depth graph of core NL4 with vertical dashed lines marking every 1000 yr. Note the question-mark at the top marking lost sediments of unknown lithology and the core catcher in the bottom with the oldest ^{14}C age. Also note that the thicker dashed line of the lower boundary of Unit 7 also marks the onset of the Eggøya tephra. **C.** Age-depth graph of core NL2. Note that Unit 4 is related to the 1954 storm surge and that the youngest ^{14}C age has been set to the mid-1950s. Also note that the oldest ^{14}C age is too old to be shown, see [Table 2](#). (For interpretation of the references to colour in this figure legend, the reader is referred to the Web version of this article.)

70.6, 78.2 and 71 cm in NL1B, NL2 and NL4, respectively, related to the lithologic descriptions in [Table 2](#) and with the age of 218 cal yr BP.

The upper part of the longest (and oldest) core NL4 shows many lithologic similarities with the other cores, while the lower sections (Units 1–6) generally differ in terms of being more fine-grained and slightly more organic. However, it bears some resemblance with the lower part (Units 1–3) of NL2, although individual units of the two cores are hard to correlate with each other. It appears that the only reliable correlation tool is the occurrence of the Eggøya tephra in the three cores. If the depth positions of the Eggøya tephra are correct, it results in the following rough stratigraphic correlations: Units 1–2 in NL1B = Unit 1 in NL2 = Unit 6 in NL4, and Units 7–10 in NL4 = Units 2–6 in NL2 = Units 3–8 in NL1B ([Fig. 4](#)). Those correlations result in approximate amounts of sediments at the three sites since the onset of deposition of the Eggøya tephra: 65.6 cm in NL1B, 68.2 cm in NL2 and 57 cm in NL4, without accounting for what may have been lost at the core tops. For example, in NL4 we know that we probably lost 25–30 cm.

4.2. Chronology

Owing to the relatively few ^{14}C dates, the presence of age reversals ([Fig. 4](#)) and the likely highly variable sedimentation rates, reliable age-depth modelling of the sequences is impossible. Instead we base the age-depth diagrams on a combination of available ^{14}C dates, the Eggøya tephra and lithological assessment of each core.

In NL1B one ^{14}C age is older than AD 1950 ([Table 1](#)), which makes it critical to trust the presence of the Eggøya tephra in Unit 3 ([Table 2](#)). The age-depth graph of NL1B ([Fig. 5A](#)) shows that the cored sediments may have an age of ~ 600 cal yr BP. If our interpolations between the Eggøya

tephra at ~ 70 cm in Unit 3 and the bottom-most and uppermost dated levels are correct, it results in a sedimentation rate of ~ 0.7 mm/yr before the Eggøya eruption and 2.7 mm/yr after the eruption. However, the highly variable lithology ([Suppl. Mat. Table 1, Fig. 4](#)) suggests that sedimentation rates may have fluctuated considerably, which our few available dates cannot capture.

In NL4 we have five ^{14}C measured sediment levels, including the sediment in the core catcher ([Fig. 4](#)). We also have geochemical data that show that the blackish sand layer, Unit 7, at 70–71 cm ([Tables 2–3](#)) is the Eggøya tephra ([Fig. 5B](#)). This time marker (218 cal yr BP) connects the lower ^{14}C dated sediments with the younger 70 cm of sediments without ^{14}C dates. The deepest dated level of the sequence is the sediments in the core catcher and this level was estimated to be 173 ± 4.5 cm, i.e. 168.5–177.5 cm. The three lowest ^{14}C ages suggest that the bottom of NL4 has an age of ~ 3000 cal yr BP. The postulated changes in sedimentation rates at 161.5, 151, 126 and 71 cm ([Fig. 5B](#)) are reflected by changes in lithology, especially observed grain-size, and the position of the ^{14}C date at 126 cm. For example, the lithology in the lower part of Unit 5 ([Suppl. Mat. Table 1](#)) is considerably more abundant in coarser layers than above. In fact, some may be tephra layers, which usually result in higher sedimentation rates. Based on the age-depth curve in [Fig. 5B](#) the sedimentation rates vary considerably: 2.5 mm/yr (units 7–10), 1.1 mm/yr (lower part of Unit 5), 0.5 mm/yr (units 2–4), 0.27 mm/yr (Unit 6 and upper part of Unit 5) and 0.2 mm/yr (Unit 1).

In NL2 we have six ^{14}C measured levels ([Fig. 4, Table 1](#)), of which one is very young (~ 10 or 65 yrs old) and one is very old (16–17 kyr BP). The young age is explained by recent high sedimentation rates since the site is close to the sea shore, and the recent disappearance of sea ice has led to the impact of storm swells on Bommen ([Fig. 3B](#)) and into the lake. The

proximal effect of the open ocean is also witnessed by the fact that the exceptional storm of AD 1954 (Barr, 2003) destroyed the American base Atlantic City situated just northeast of NL2. We consider it likely that the storm was the agent behind deposition of the coarse and fining upwards sediment sequence of the upper part of Unit 4 (Fig. 5C). The old age is more difficult to comprehend since it is the only material dated to before the Late Holocene. If the dated material is of primary origin the age would also imply a very long hiatus in a seemingly dynamic sedimentation environment. We suggest that this anomalous date stems from the presence of reworked plant material, eroded from sediment exposures along incoming streams within the catchment. The plant material may either originate from a mix of Holocene and older interglacial material or from pioneer vegetation after the area had become ice-free, some time after LGM, and does thus not date the surrounding sediments. The remaining dates vary between ~100 and 700 cal yr BP with fairly large uncertainties and they are not in a stratigraphic order (Fig. 5C). This makes any age-depth graph speculative but our attempt is supported by geochemical analyses that show that Unit 2 (Suppl. Mat. Table 1) at 78.2–77.5 cm is most likely tephra from the AD 1732 Eggøya eruption (Table 2). This results in an age of ~400 cal yr BP for the bottom part of Unit 1, although the 93–96 cm age (Table 1) implies an older age for the bottom of core NL2. However, in a dynamic arctic sedimentary environment like Jan Mayen one may expect reworking of older organic material, for example from the fluvial fans like the one in Tornøedalen (Fig. 3C). We therefore regard younger ages as more reliable. Based on the age-depth graph (Fig. 5C) the resulting sedimentation rates have varied between ~1.4 mm/yr before the Eggøya eruption, 0.6 mm/yr after the Eggøya eruption until the 1954 storm. Unit 4 was possibly deposited more or less instantaneously by the storm, and the uppermost ¹⁴C date implies that the onset of Unit 5 corresponds either to the mid-1950s or end of the 2000s (Table 1). We regard the former alternative more likely since it seems to date the storm very well. This results in >15 cm being deposited since the mid 1950s, i.e. a sedimentation rate of >2.5 mm/yr.

In general, it is challenging to create a detailed and fully trustworthy chronology with the type of sediments we find in Nordlaguna with possibly highly variable sedimentation rates, even within individual units, and a very low content of organic material prohibiting dense and reliable ¹⁴C dating. Regarding the highly variable sedimentation rates, especially in connection with the Eggøya tephra, we have to consider vertical uplift as an important agent. For example, Larsen et al. (2021) demonstrated vertical uplift on the order of 14 m in Wilczekdalen Valley during the volcanic eruption in AD 1732. This was postulated as the main driver behind the isolation of the Nordlaguna basin. Further evidence of recent uplift is revealed by georadar profiles across Bommen and in the other valleys entering the lake (Larsen et al., 2022). Thus, increased sedimentation rates after the Eggøya tephra (Fig. 5A–B) may account for increased sediment input during uplift and that the lake became landlocked and as such a more efficient sediment trap.

4.3. XRF core scanning data and cross-correlation of the sequences

The high-resolution elemental results of the three cores, measured by XRF core scanner, and transformed by a center log ratio (clr), allow us to assess the cross-sequence correlations suggested above as well as give us an idea about the changing conditions within the lake. Before we do this however, we should consider the relative position of each of the sequences within the lake as this impacts how we look at the core data (Fig. 2). NL1B is situated in the deepest southwestern part of the basin, fairly close to incoming streams from the south and east, NL2 is situated close to the Bommen barrier and the open sea, and NL4 is situated in the most central and deepest area of the lake. We therefore expect that NL1B more reflects fluvial erosion of the surrounding catchment with different source areas while NL2 should show strong direct impact from the sea and its erosive products. Conversely, NL4 reflects the most calm, distal and fine-grained sedimentation in the lake with only one main source area east of the coring site (Figs. 2 and 3C). These differences are already indicated from the

lithology of the different sequences and explains why the sediments in NL4 were easiest to penetrate. Therefore, NL1B and NL2 may have registered some local aspects of NL's history, such as erosional and sudden sedimentary events, but it seems appropriate to use NL4 for its longer history and its continuous sedimentation.

To test the cross-sequence correlations we made using the lithological information, we plotted some of the more common elements, Cl, K, Ca and Ti, but also Br (Fig. 6A–C). It shows partly a similar general pattern of the five elements across the cores with Br and Cl displaying the least positive and Ca highest values in each core. In contrast to NL1B, the elemental profiles of NL2 and NL4 suggest a clear shift in the system, around 64 cm and 72 cm, respectively. The elemental response after this shift shows a distinct decline in Br values and higher values of K, Ti and Ca (Fig. 6B and C). Another noteworthy feature is that NL4 displays higher variability before this shift (Fig. 6B), while the opposite is true with NL2, especially between 64 and 27 cm (Fig. 6C), and NL1B has rather stable K, Ti and Ca values throughout the profile, while Br and Cl are more variable (Fig. 6A).

The Eggøya tephra is a lithostratigraphic marker we can use to compare the chemo-stratigraphy and this suggests that elemental patterns vary in the three cores at the time of tephra deposition. In NL1B we note minima in K, Ti and Ca values and a Cl peak at the Eggøya tephra at 71 cm and with similar features between 66 and 63 cm (Fig. 6A). In NL4 the position of the Eggøya tephra is slightly above where we see large elemental shifts, while similar profile shifts in NL2 occur 13–15 cm above the Eggøya tephra. A similar feature is seen in NL2 where the Eggøya tephra coincides with distinct minima in K, Ca and Ti and a maximum in the Cl values at 78 cm (Fig. 6C), but nothing comparable can be seen in NL4 (Fig. 6B). Because of these inconsistencies between the cores' elemental profiles and the position of the Eggøya tephra, the chronologies of the three cores may be ambiguous. However, we should take into account that the eruption was observed on May 17th 1732 (Anderson, 1746) with tectonic movements around the lake (Larsen et al., 2021) and in all likelihood the lake was still ice-covered. These factors may have created differences in how and when the tephra was deposited at the core sites. However, whatever the reasons are for the inconsistencies, without good ¹⁴C dating we need to rely on the tephra (geochemistry) as a time marker.

The elemental profiles in Fig. 6A–C imply that the cores partly contain different types of sediments or stratigraphic units although they were deposited more or less synchronously. One reason for the differences may be related to grain-size variations/changes and different sediment sources, resulting in diverse elemental signals. In order to achieve a better understanding of the sedimentary environment of the basin a large number of elemental ratios have been calculated and tested. The log(Zr/Rb) ratio (Fig. 7) is affected by both changes in grain size and source and we note fairly constant ratios in the three cores except for the lower part of NL4, below the Eggøya tephra, where the ratios are higher and much more variable. This gives an impression that the lower part of NL4 contains sediments that are not found in the other cores. The few samples analyzed for mean grain-size, also shown in Fig. 7, show substantial changes, as also described in Suppl. Mat. Table 1. The coarse sediments in NL2 above 64 cm are clearly shown by the grain-size (Fig. 7), but the ratios also show a shift, which may imply that changes in both sediment source and grain-size occur above 64 cm. It is therefore likely that the fairly stable Zr/Rb ratios in NL1B and above the Eggøya tephra in NL4, indicate no large change in the source of the sediments; both primary and reworked tephra material has possibly been a constant dominant source. It also indicates that the source of the sediments below the Eggøya tephra in NL4 is partly different than in the other cores which is in agreement with the suggested age models and the older sediments captured in NL4.

4.4. Paleoenvironmental development as revealed by Lake Nordlaguna

One of the main aims of this study is to establish if Nordlaguna has at one time been connected to the sea and if so, establish when this may

Table 3

Results from a Principal Component Analysis (PCA) of the clr transformed, 10 smoothed, data from NL4, but without sulphur and the transition metals Ni, Cu and Zn. Here we show the elemental scores for the four strongest PCA axes, Factor 1–4, and the variance explained by each factor as well as accumulated variance. Note that positive (negative) elemental scores higher than 0,4 (lower than -0,4) are shown in red and blue, respectively. The sample scores of these elements are shown in Fig. 12.

	Factor 1	Factor 2	Factor 3	Factor 4
Explained variance (%)	29	27	22	13
Cumulative percentage (%)	29	56	78	91
Si	0,36	0,39	0,80	0,00
Cl	-0,72	-0,17	-0,59	-0,23
K	0,74	0,39	0,47	-0,11
Ca	0,25	0,62	0,61	0,31
Ti	0,50	0,44	0,57	0,33
Mn	0,42	0,76	0,17	0,27
Fe	-0,05	0,21	0,08	0,93
Br	-0,57	-0,62	-0,46	-0,21
Rb	0,94	0,13	0,15	-0,10
Sr	0,58	0,48	0,35	0,37
Zr	-0,09	-0,90	-0,32	-0,13

have occurred. In order to investigate any marine influence on the sediments, the presence of Br can be used. It has been used to quantify marine organic matter (e.g. Caley et al., 2011) and to distinguish between marine and freshwater conditions (e.g. Mayer et al., 2007; McHugh et al., 2008). Bromine (Br) is the 10th most common element in sea water and much less common in terrestrial environments compared to other common marine elements, e.g. Cl, Na, Mg, Ca and K. We note a distinct drop in Br values in NL4, and a small drop in NL1B, at the Eggøya tephra (Fig. 6). In NL2 a large drop is found 15 cm above the Eggøya tephra at the onset of Unit 4, the storm deposit, which may be regarded as remarkable if Unit 4 has a dominantly marine origin. However, the coarse nature of Unit 4 and the fact that most of Unit 4 may have originated from the sub-aerially exposed Bommen barrier may explain the drop.

In contrast to Br, Zn has low abundances in marine environments (Rothwell and Croudace, 2015), and we notice a general trend in our data of increasing Zn when Br decreases. The correlation between Br and Zn (Pearson correlation coefficient) in all three cores are negative, with r values from -0.29 ($n = 4078$) in NL2 to -0.30 ($n = 2960$) in NL1B and the strong negative value of -0.89 ($n = 7554$) in NL4. The latter is also the core showing the strongest evidence of previous marine impact. We use the $\log(\text{Br}/\text{Zn})$ ratios as an indicator of marine influence on Lake

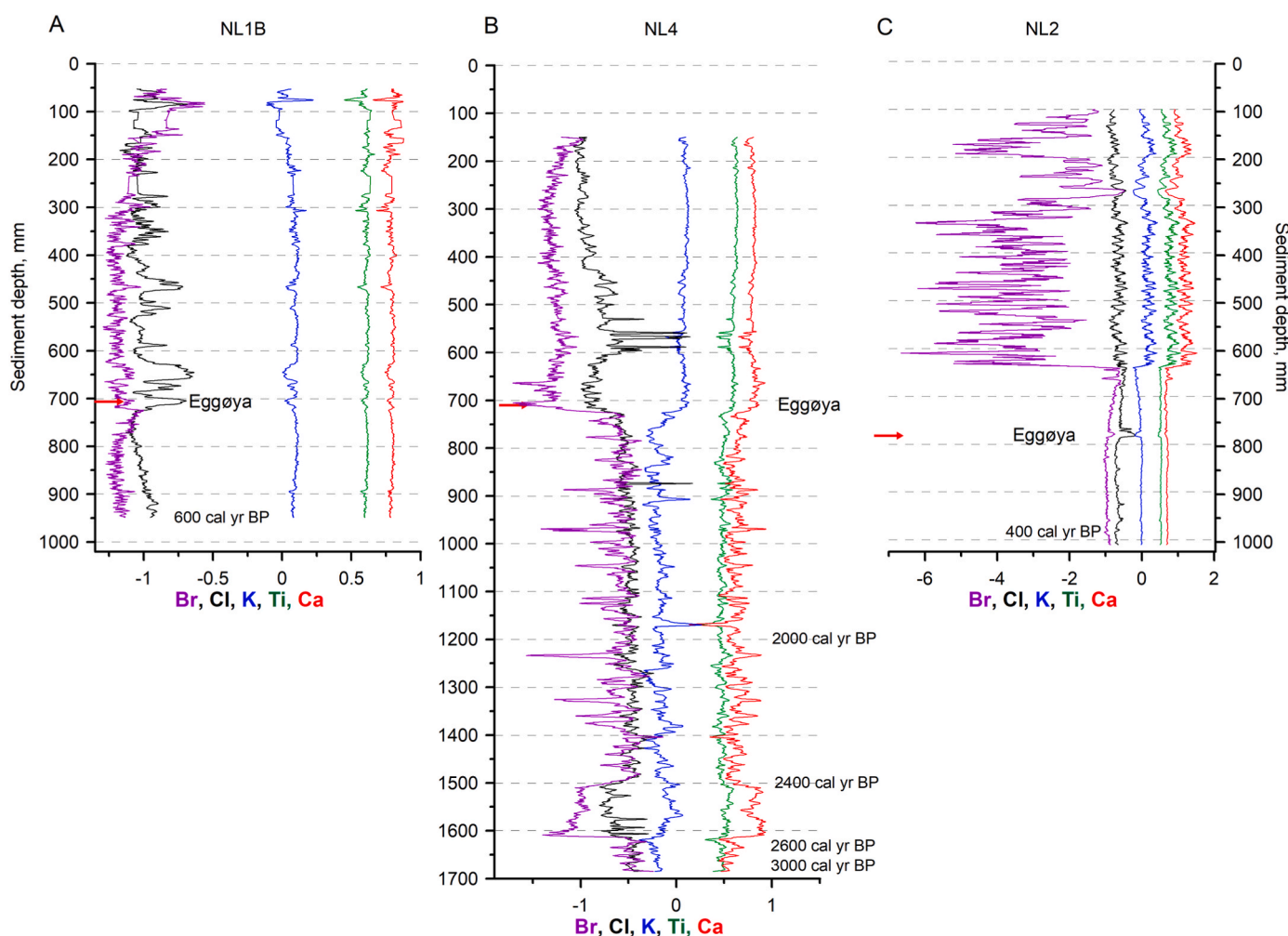


Fig. 6. Center log ratio (clr) transformed XRF values for four of the most common elements, Cl, K, Ti and Ca, from the three core sites, grouped from southwest to northeast. The values indicate how relatively common the elements are in relation to each other. The precise position of the Eggøya tephra is marked by red arrows and also shown as text. **A.** Clr transformed values for core NL1B. Note that the position of an estimated age of 600 cal yr BP is marked. **B.** Clr transformed values for core NL4. Note that the positions of four estimated ages, from 2000 to 3000 cal yr BP, are marked. **C.** Clr transformed values for core NL2. Note that the position of an estimated age of 400 cal yr BP is marked. Also note the different x-axis scales. (For interpretation of the references to colour in this figure legend, the reader is referred to the Web version of this article.)

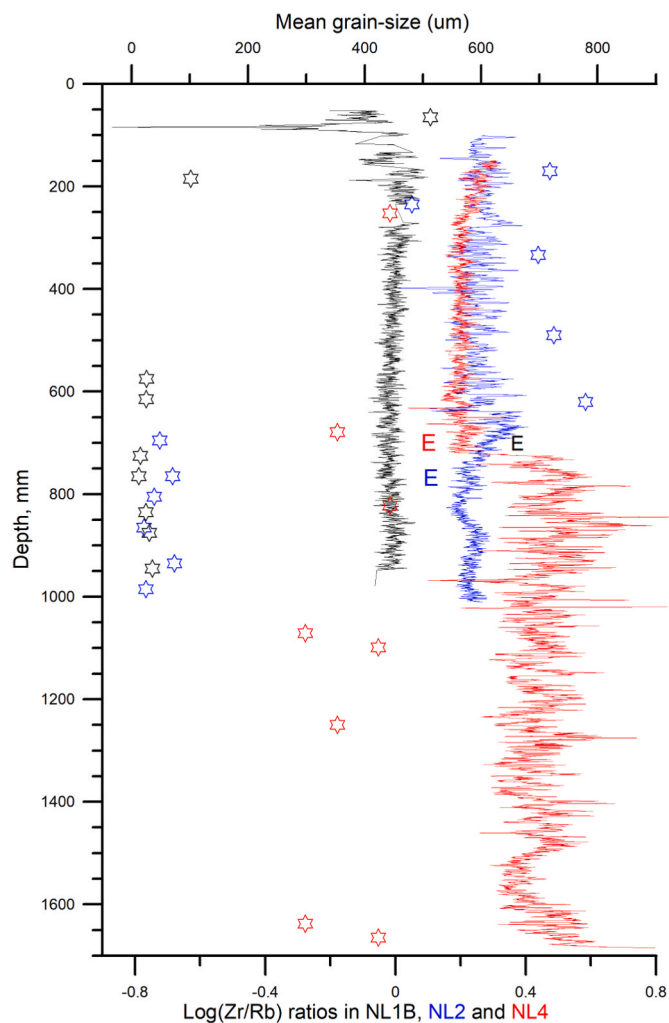


Fig. 7. Log(Zr/Rb) ratios, based on XRF data from NL1B (black), NL2 (blue) and NL4 (red), compared with >20 samples for mean grain-sizes from the three cores, shown with black, blue and red stars. (For interpretation of the references to colour in this figure legend, the reader is referred to the Web version of this article.)

Nordlaguna (Fig. 8). The log(Br/Zn) values in NL1B are fairly constant and less variable than in the other cores (Fig. 8), which indicates that the core reflects a situation similar to today's with an isolated lake basin. We note however, slightly falling log(Br/Zn) ratios at ~72 cm, i.e. around the Eggøya tephra, which may be a hint of marine conditions before that. The falling log(Br/Zn) ratios above 64 cm and 72 cm in NL2 and NL4, respectively, imply that marine influence ceased at those depths. We also note a distinct shift to lower log(Br/Zn) ratios in NL4 between 150 and 160 cm (Fig. 8), dated to c. 2400–2600 cal yr BP, implying a phase of less marine, perhaps only slightly brackish conditions. The assumed shifts between marine and brackish/more fresh-water like conditions in NL4 are also mirrored by the magnetic susceptibility curve from NL4 (Fig. 8): during periods with a more open connection between the lake and the sea we note higher magnetic susceptibility. This possibly reflects the fact that during such circumstances a larger amount of fine-grained material, clay-fine silt, with lower magnetic susceptibility (Björck et al., 1982) left the basin as suspended material, concentrating the susceptibility signal in the basin, while the opposite was true during conditions when the inflow of particles (clay-gravel) from the surroundings of the lake, stayed within the basin when it was more or less closed. This diluted the susceptibility signal, which we see in the top of the core after the isolation but also at 1500–1600 mm (Fig. 8), i.e. around 2500 cal yr BP.

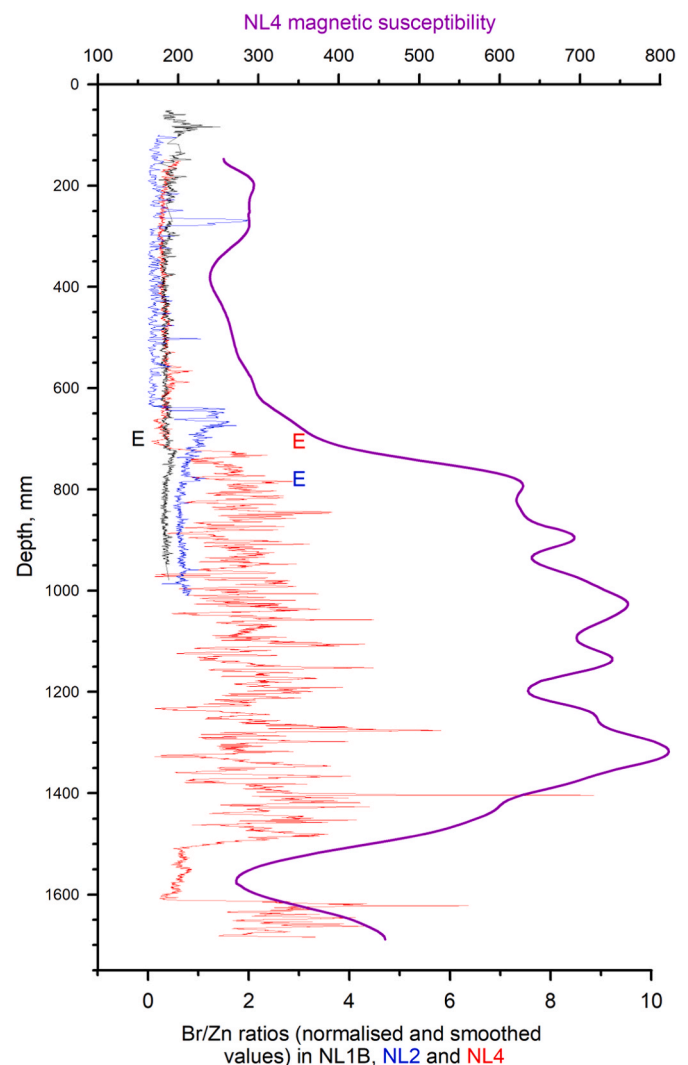


Fig. 8. Br/Zn ratios based on the raw normalized and smoothed XRF data from NL1B, NL2 and NL4. The purple curve shows the magnetic susceptibility values in NL4. Note that the positions of the Eggøya tephra in the different cores are indicated by a coloured E. (For interpretation of the references to colour in this figure legend, the reader is referred to the Web version of this article.)

Regarding the chronology of the cores, it is noteworthy that the Eggøya tephra is situated approximately at the Br shift in NL4, but occurs 10–15 cm below the same shift in NL2. This indicates that the lithostratigraphic positions of the Eggøya tephra in the three cores may not be perfectly constrained; it may be possible that we have not found the first occurrence of the Eggøya tephra in all cores. This is further supported by the log(Si/Ti) ratios (Fig. 9), which can partly be a signal for biogenic silica (diatoms). They show distinctly rising ratios in NL2 10–15 cm above the Eggøya tephra, while rising ratios in NL4 coincide with the Eggøya tephra, but are thereafter followed by oscillating values, which is similar to NL1B (Fig. 9). Similar discrepancies between the cores and the position of the Eggøya tephra are seen with the log(Ca/Sr) ratios (productivity, source change). In NL2 the ratios are fairly constant in the lower section but rise 10–15 cm above Eggøya (Fig. 10), and stay high but variable, while they display a highly variable pattern before the tephra in NL4 but are fairly constant above the tephra. NL1B shows fairly stable ratios, but with higher variability after the tephra, just like in NL2 but less chaotic. From these comparisons one can conclude that the main shifts of these ratios in NL2 occur at the onset of Unit 4, the supposed storm deposit, and not at the Eggøya tephra as in NL4 and partly also in NL1B.

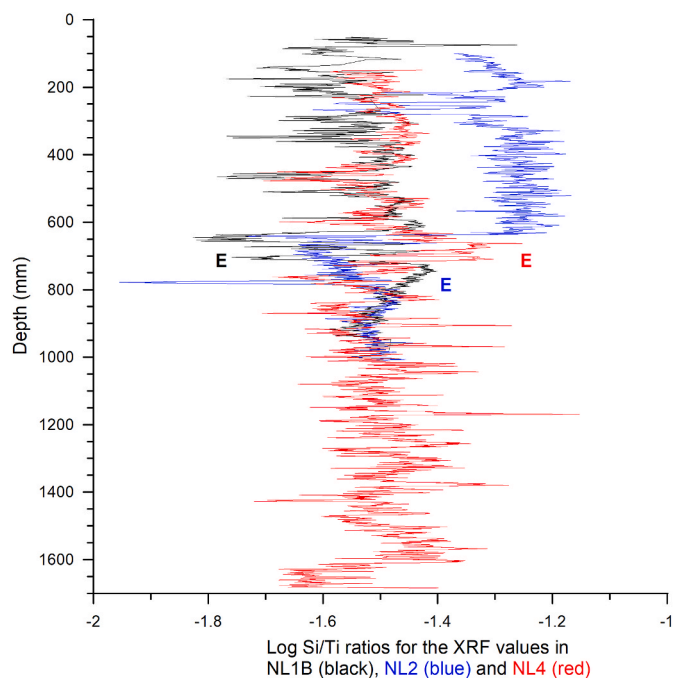


Fig. 9. Log(Si/Ti) ratios, based on clr transformed XRF data from NL1B (black), NL2 (blue) and NL4 (red). Note that the positions of the Eggøya tephra in the different cores are indicated by a coloured E. (For interpretation of the references to colour in this figure legend, the reader is referred to the Web version of this article.)

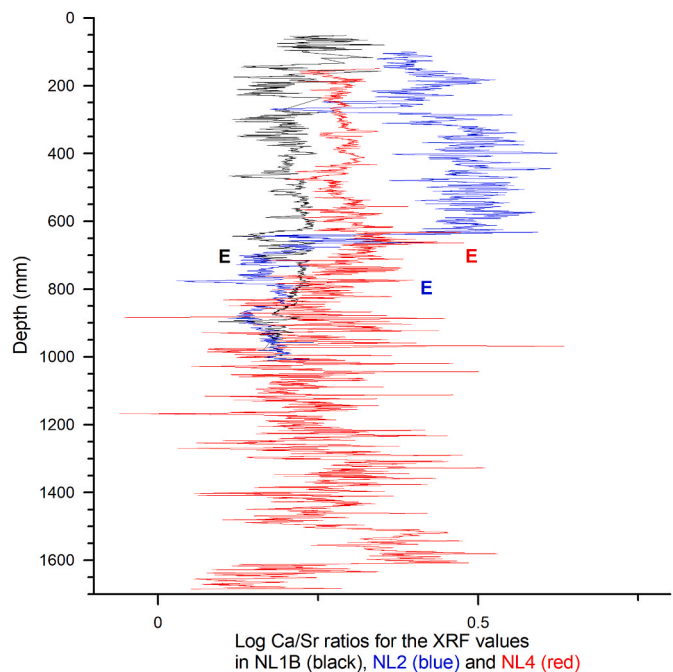


Fig. 10. Log(Ca/Sr) ratios, based on clr transformed XRF data from NL1B (black), NL2 (blue) and NL4 (red). Note that the positions of the Eggøya tephra in the different cores are indicated by a colored E. (For interpretation of the references to colour in this figure legend, the reader is referred to the Web version of this article.)

Considering the fact that NL4 is the longest and oldest core with a possibly continuous sedimentation and it is centrally positioned in the lake away from a more proximal influence of the fluvial inputs (NL1B) or the beach barrier (NL2), we focus on this core in order to build a

temporal picture of the paleoenvironmental development at NL over the last ~3000 years. In order to acquire a better understanding of the elemental suite we have carried out a Principal Component Analysis (PCA) on the clr transformed data, excluding S and transition metals Ni, Cu and Zn. We have also used the age-depth curves to plot the data versus age.

Before we discuss the PCA data from NL4 we should, however, shortly mention the PCA results from the other cores. We note that the PCA data from NL1B, not shown here, show that the variance covered by the first four PCA axes is very similar; while the PC1 covers 24.3% of the variance PC4 covers 21.1%. This means that any combination of the first four PC axes can be used to interpret the XRF data. When it comes to NL2, and a chronology based on the assumptions that the Eggøya tephra occurs at 78 cm and that Unit 4 corresponds to the 1954 storm event, it shows that PC1 covers 85% of the variance. It also shows that Br and Cl dominate the XRF signal until the impact of the 1954 storm event (Fig. 11). The plot shows that two shifts occur in the data: at the Eggøya tephra, shown by PC2 but only covering 10% of the variance, and at the onset of the supposed storm event, shown by both axes. The fact that a “marine signature” dominates until the storm surge, with strongly negative Br loadings for PC1 and strongly positive Cl loadings for PC2 (Fig. 11), may be surprising in the light of the other cores. We speculate that this may be related to the proximity of the sea to NL2, with a potential for continuous marine inwash until the storm built up/ resulted in a more efficient Bommen barrier in the north.

In NL4 principal component 1 (PC1) explains 29% of the variance in data and is associated with K, Ti, Rb and Sr on the positive and Cl and Br on the negative (Fig. 12 and Table 3). PC2 explains 27% of the variance in the data and is associated with Ca and Mn on the positive and Br and Zr on the negative. PC3 and PC4 account for 22% and 13% of the data

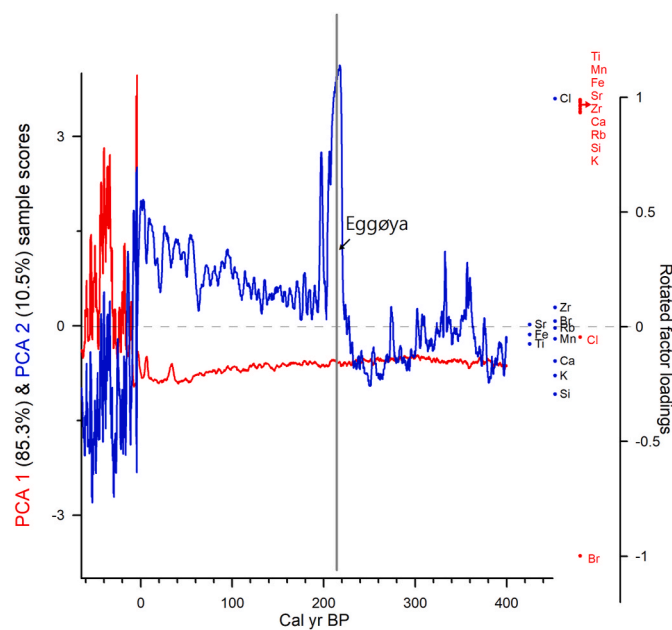


Fig. 11. Principal component analysis (PCA) of the clr transformed XRF data (11 elements) from NL2, displaying the result of the first two axes, PCA1 (red) and PCA2 (blue), covering 95.8% of the total variance. Note that the PCA values of each sample (left y-axis) are related to cal yr BP (x-axis) and that the rotated factor loadings of the 11 elements are shown as red (PCA1) and blue (PCA2) dots related to the y-axis to the right, and that also the signatures for the PCA1 elements are shown in red. Note especially that 9 of the elements for PCA1 all have high positive factor loadings and cluster together up to the right, while the loadings for Cl and Br are negative. Also note that the position of the Eggøya tephra is marked by a grey column. (For interpretation of the references to colour in this figure legend, the reader is referred to the Web version of this article.)

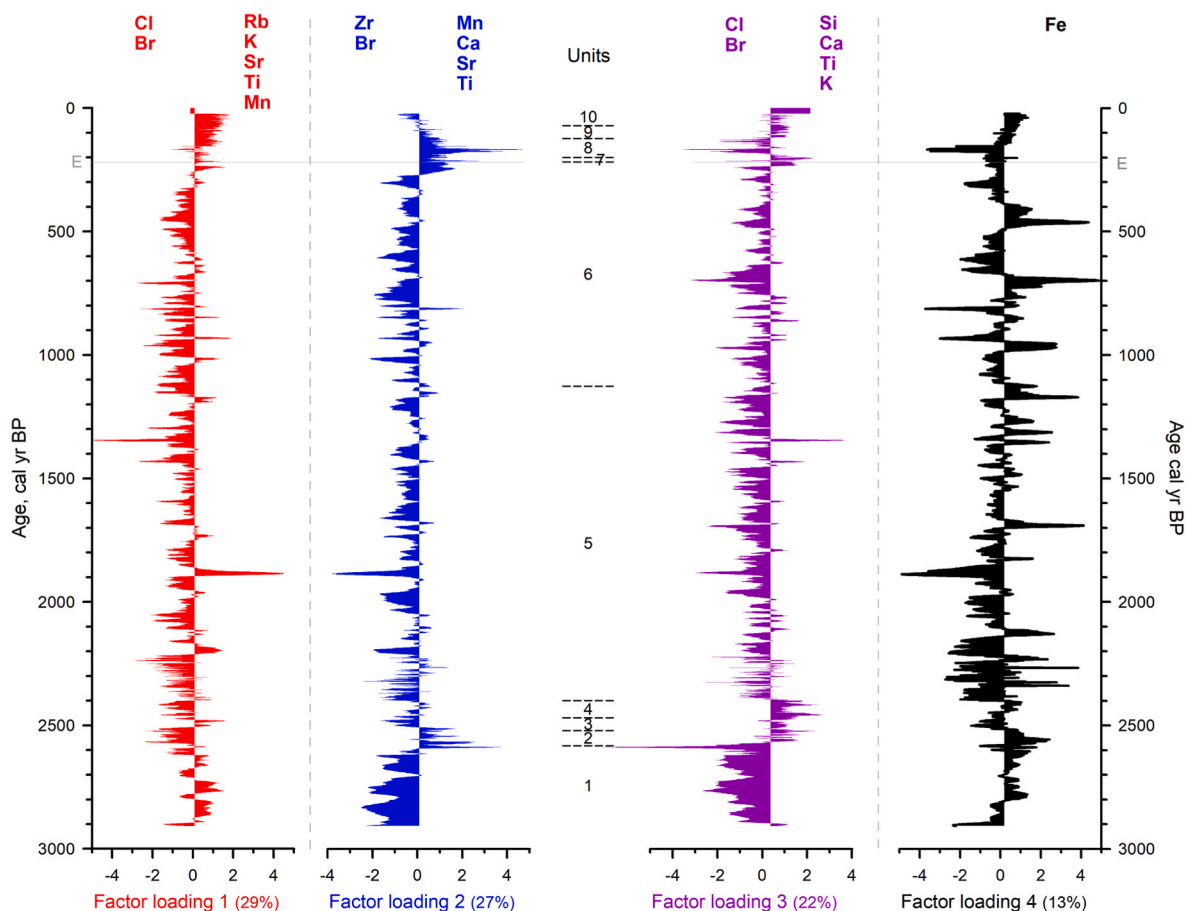


Fig. 12. Results from principal component analysis (PCA) of the clr transformed XRF data (11 elements) from NL4, displaying the temporal development of the sample scores of the four strongest PC axes (factor loadings), PC1 (red), PC2 (blue), PC3 (purple) and PC4 (black), in total explaining 91% of the variance. Note that the elements with strongest positive and negative scores for each axis (Table 3), i.e. ≥ 0.4 (≤ -0.4), are shown above the sample scores for each axis in the order of strength. The lithological units of NL4 plotted versus cal yr BP shown in the center. Note that the Eggøya tephra occurs at the onset of Unit 7 and is displayed as a thin grey line through all four factor loadings and with an E at the y-axes. (For interpretation of the references to colour in this figure legend, the reader is referred to the Web version of this article.)

variance, respectively. PC3 is mainly associated with Si but also Ca and Ti on the positive and Cl on the negative. PC4 is strongly linked to the behavior of Fe. By examining changes in the PC by plotting their factors scores by age and by comparing with the sediment and the lithostratigraphy, a few key processes can be identified (Fig. 12).

PC1 appears to present the balance between marine and terrestrial sources with the grouping of marine associated elements Br and Cl (e.g. Caley et al., 2011) on the negative and lithogenic elements Rb, K, Ti and Sr on the positive. The pattern of PC1 indeed mimics that of $\log(\text{Br}/\text{Zn})$ with the major shift towards the positive occurring at the Eggøya tephra (Fig. 8). Prior to this point the values are predominantly negative, consistently so between e.g. 2200–1900, 1850–1250 and 600–300 cal yr BP, suggesting a more or less strong connection with the sea for much of the record (Fig. 12). The supposed isolation of Lake Nordlaguna accords well with the conclusion by Larsen et al. (2021) that a connection with the sea, via Wilczekdalen, was closed by volcano-tectonic uplift at the time of the Eggøya eruption. It is interesting that some more distinct, often short-lasting, positive peaks occur in the core implying less marine impact, especially in the bottom of the core, for example, between ~ 2900 and 2700 , at ~ 2200 and at ~ 1900 , 1200 , 1050 and 950 cal yr BP (Fig. 12). If the Br and Cl values are true marine signals it indicates that the conditions in the basin have continuously fluctuated, perhaps as a consequence of a more or less efficient Bommen barrier between the sea and the basin, relative sea level change and the impact of sea spray and washed-in water during stormy conditions. It is also possible that there could have been short partly isolated phases of the lake from the sea

through for example temporary impediments in the watercourse between the lake and the sea, but still with some marine impact over the Bommen barrier (Fig. 3B), creating at least slightly brackish conditions. The seemingly more common marine impact after 600 cal yr BP may be the effect of increased storminess during the Little Ice Age, at least during summers with less sea ice, perhaps partly destroying the Bommen.

PC2 shows more positive values at those depths with darker sediment present and where tephra have been identified during core description (e.g., Units 2, 7 and 8). If this is the case it would mean that in the more coarse-grained tephra being transported to NL, Ca and Mn is found in higher concentrations than the rest of the catchment material. Indeed, Br and Zr plot on the negative for PC2. Br, in addition to being indicative of marine influence is also associated with organic matter in lakes (Guevara et al., 2019) while Zr is often enriched in finer ($<150 \mu\text{m}$) (Sjöström et al., 2022) and silt sized fractions (Taboada et al., 2006). As such, more negative values of PC2 could represent a type of local background with local weathering and the influx of finer grained material and organic matter from the catchment.

PC3 is loaded most heavily by Si but also Ca and Ti on the positive with Cl and Br on the negative (Table 3, Fig. 12). While Si and Ca can be associated with biological productivity in the lake and the catchment, the association with Ti would suggest that PC3 is linked to some type of minerogenic process. The factor scores of PC3 by age are fairly similar to PC1 and PC2 for Units 5 and 6 (2400–220 cal yr BP), with the negative scores supporting the dominating marine impact for this part of the

sequence that we invoked for PC1. The main exceptions with positive values are found in Units 2–4, 7 and 9–10. Apart from the negative scores in Units 5–6 we also find them in Units 1 and 8 (Fig. 12). Whether this is related to marine influence or not is difficult to evaluate since we know, with some certainty, that Unit 8 is not marine. However, the strongly negative PC3 peak in Unit 1, followed by positive values, is reminiscent of the $\log(\text{Br}/\text{Zn})$ ratios (Fig. 8), and we find it likely that this represents salinity changes. We therefore conclude that these partly contradicting data evoke that PC3 expresses not only a potential signal of sediment source changes, but also of marine influence.

PC4 represents almost only the behavior of Fe which makes identifying the processes driving Fe variability difficult to establish. When we compare PC1 and PC4 it shows that samples with highly negative scores for PC1, dominated by Br and Cl, often corresponds to positive scores for PC4, dominated by Fe. This may be an indication of changes in redox conditions; could more inflow of saline water have caused anoxia at the bottom of the lake as a result of more dense, salty water? This assumption is supported by the abundant occurrence of blackish layers of non-tephra origin in Unit 5, peaks in PC4 and the occurrence of S and

C (Suppl. Mat. Table 1); the latter being less decomposed due to anoxic conditions. We note the same, but less distinct, pattern in the upper part of Unit 6; a distinct Fe peak and more blackish layers are noticed before the supposed lake isolation.

5. The marine impact on Lake Nordlaguna: a discussion

Our XRF data demonstrate the presumed isolation of NL around the time of the Eggøya tephra at 218 cal yr BP (Fig. 12), when a former marine connection between the southeastern corner of NL and the Maria Musch Bay (Figs. 2 and 13) experienced extensive tectonic uplift (Larsen et al., 2021). This resulted in the isolation of NL and subsequent creation of today's land-locked basin. The XRF/PCA data in NL4 from the period before this fairly dramatic event are not straight-forward regarding the marine impact. We have mainly used the elements with negative loadings (Br and Cl) for PC1 for interpreting this impact and explained the negative loadings of Zr, Br and Cl in PC2 and PC3 (Fig. 12) with additional likely processes, except for the lowest part in NL4 (Units 1–4) where we reason that the large shifts in PC3 loadings and in the log

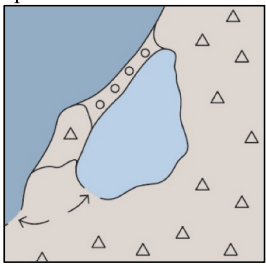
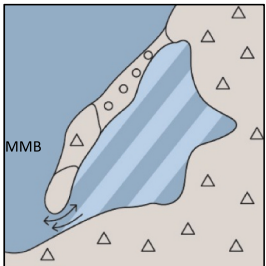
Acc. to Larsen et al. (in press)	This work, based mainly on the NL4 site	Interpretations
Landlocked lake from AD1732 due to tectonic uplift 	AD 1732 – present <i>Lithology and chronology:</i> High sedimentation rate (~2.5 mm/yr) after 1732 (Eggøya tephra) <i>Itrax-XRF:</i> Transition to freshwater dominated environment and terrestrial mineral input dominated by reworked volcanic (tephra) material	Landlocked lake with minor marine impact; ocean wave wash over the Bommen beach barrier and penetration of saline water through the same barrier
Ca. 6 ka – AD 1732 Marine bay/lake, connection with the marine environment through an outlet to Maria Musch Bay (MMB)	Ca. 2.4 ka – AD1732 <i>Lithology and chronology:</i> Variable sedimentation rates (0.25-1.25 mm/yr) <i>Itrax-XRF:</i> Dominating marine environment/ marine mineral input, some short-lasting more terrestrial phases	Marine bay/ intervening fresh-water pulses caused by varying amount of ocean water being able to enter NL over the Bommen barrier and/or through the Maria Musch inlet
	Ca. 2.6 ka -2.4 ka <i>Lithology and chronology:</i> Low sedimentation rate (0.6 mm/yr) <i>Itrax-XRF:</i> Terrestrial mineral input/ freshwater dominated environment with some marine influence	Lake phase, isolation caused by creation and closure of the Bommen barrier and possibly by land uplift.
	Ca. 3 ka – 2.6 ka <i>Lithology and chronology:</i> Generally low sedimentation rate (0.3 mm/yr) <i>Itrax-XRF:</i> Marine mineral input/dominating marine environment	Marine bay, possibly caused by a higher relative sea level

Fig. 13. The general development of Lake Nordlaguna, according to Larsen et al. (2022) to the left, and with a more detailed account based on this work, and with some more general environmental interpretations to the very right. Note that the Maria Musch Bay outlet is marked with MMB and arrows.

(Br/Zn) ratios (Fig. 8) may indicate distinct salinity changes. Altogether this implies that the extent of the marine-freshwater contact oscillated between ~220 and 2400 cal yr BP (Figs. 12 and 13), and with a narrow but probably main contact with sea to the Maria Musch Bay (Fig. 2). This setting seems to have been preceded by a ~200 year long phase of more isolated conditions between 2400 and 2600 cal yr BP, which in turn seems to have been preceded by a state with significantly more marine impact since the start of the sequence at ~2900 cal yr BP.

Since we have no information about raised shore lines and relative sea level changes, and the long-term interaction between isostasy and eustasy on Jan Mayen, we can only speculate about what led to these changes. We note that the change from Unit 1 to Unit 2 at 151 cm/2600 cal yr BP is very sharp in terms of the elemental data (PC3 in Figs. 12 and 8), which is also indicated by the erosional sharp contact between the units (Fig. 4; Suppl. Mat. Table 1). We thus seem to have a rapid change at ~2600 cal yr BP from a setting influenced by more or less marine water (Unit 1) to a more fresh-water dominated basin (Unit 2). In fact, the lithology and general nature of Unit 1, dated to 2900-2600 cal yr BP (Fig. 5B), suggest a marine character, more marine than what is seen in any other units/cores, and display the highest S and C values (Suppl. Mat. Table 1). This change thus ends up with Units 2-4 in NL4, which are dated to 2600-2400 cal yr BP with seemingly more freshwater impacted sediments, but possibly less than after the final isolation. This change into less marine conditions could, e.g., be explained by a gradual ceasing and eventual end of the local glacial isostatic uplift. During the end of this, possibly very slow regression, the Bommen barrier could have been formed by a combination of long-shore drift and landward roll-over processes. This implies that marine water could have entered NL over both the Bommen and through the Maria Musch inlet during the first marine phase of perhaps slightly higher sea level, ending up with the first slightly isolated phase at 2600-2400 cal yr BP; perhaps a consequence of the final isostatic uplift. However, it is also possible that the 2900-2400 cal yr BP development with changing relative sea levels could be a continuation of a long history of volcano-tectonic movements changing the position and altitude of the sill of NL over time; something that seems to have happened when NL came into today's land-locked position (Larsen et al., 2021).

Since 2400 cal yr BP we believe that relative sea level has been fairly stable. In spite of the obviously oscillating pattern between more or less marine conditions 2400-200 cal yr BP (Figs. 8 and 12) NL has, in all likely-hood, never been a basin with fully marine or fresh-water conditions; the impact of fresh surface- and ground-water will always be significant and the present seepage of salt water through and over the Bommen barrier (Fig. 3B) shows that NL, in spite today's land-locked situation, have slightly saline water. It is therefore reasonable to conclude that NL has experienced more or less brackish conditions during the last ~3000 yrs. The reason for the oscillating conditions 2400-200 cal yr BP we think may be related to the fact that the Bommen barrier might have experienced more or less wave eroding phases, and together with sill changes in the Maria Musch inlet allowing more or less sea water to enter the NL basin, until the final isolation at ~220 cal yr BP.

With respect to today's Arctic char population, and with the knowledge that this species spawns in brackish or fresh water, our data indicate that there have been many opportunities for Arctic char to enter the lake; perhaps even throughout most of the period. They need at least one true inlet to enter the basin, since it is highly unlikely that they have been brought-in by occasional storm events. Therefore they must have entered NL by the Maria Musch passage and perhaps also by an earlier inlet through the Bommen barrier, e.g. when sea level might have been slightly higher than today. Since we have no data on the salinity of NL during the different pre-isolation phases and we do not know in detail what maximum salinity Arctic char can manage to be able to spawn in, it is tempting to speculate that they first arrived to NL when conditions seem to have fluctuated between almost fresh and brackish water, i.e. between 2600 and 2400 cal yr BP. It is also possible that they arrived

during the "oscillating period" 2400-200 cal yr BP as long as the inlet was open. This means that we can at least conclude that our data imply that the last phase with a possibly open inlet that later closed, trapping the fish in NL, possibly occurred slightly before the final isolation during the Little Ice Age (see PC1 in Fig. 12), which implies that today's Arctic char population may be at least several hundred years old, but perhaps even much older.

6. Conclusions

One can conclude that a major challenge with the Lake Nordlaguna (NL) sediments is that volcanic material has "contaminated" and masked most of the other environmental elemental signatures in the sediments. Although a number of primary ash fall-out layers most likely occur in the lake sediments, reworked volcanic material, from both glacial and glaciofluvial deposits, bedrock and tephra material, possibly constitutes the dominating source of the NL sediments. This has created a mix of elemental signatures from a vast amount of primary sources as well as local variations in terms of how the material has been transported, e.g. distal vs proximal, from around the lake and to the lake bottom. Additionally, during the corings from the lake ice it became obvious that the lake ice is covered by a more or less thick layer of sandy-silty sediments (Fig. 3D), most of it possibly originating from the Bommen barrier as a combination of marine erosion and wave-wash onto the barrier followed by water- and eolian-transport to the lake ice. Depending on dominating wind directions before the spring-melt, different parts of the lake ice would have varying amount of sediment with variable grain-sizes to end up on the lake floor when lake ice melts. Altogether this has created an unpredictable sedimentation pattern and this irregularity has become evident when we compare the elemental profiles from the three sediment cores; each core has its own history and not even the supposed marine influenced conditions show up as a common signal in the three XRF data sets.

The oldest sediments retrieved from the NL lake originate from the ~154 cm long core NL4 (excl. core catcher and lost sediments in the top), cored in the central part of the lake in 30 m of water. By ¹⁴C dating they are found to be ~3000 cal yr BP old, significantly older than the two other studied cores, and was therefore the main focus of the study. The almost pure minerogenic material of the sediments, usually dominated by the silt fraction, have made any paleoenvironmental reconstruction troublesome. However, the elemental content of the cores were measured, in high-resolution, by an XRF scanner. By different statistical methods it was concluded that the results could be used to investigate to what degree the lake, situated a few meters above sea level, was influenced by marine water. This is of special interest since Arctic char has been trapped in the lake.

We find that NL has been influenced by marine water over the last ~3000 years, creating more or less brackish conditions. Apart from today's land-locked situation, without a regular open lake-ocean connection, but still with some salt water influence, the lake was partly isolated between 2600 and 2400 cal yr BP. Before this phase the lake had its most marine influenced stage for 300-400 years ending up with a sudden transition to a partly isolated state. After 2400 cal yr BP the lake has oscillated between more or less brackish conditions, until the final isolation at ~200 cal yr BP. It is most likely possible for Arctic char to have used NL for spawning for a long time, perhaps during most of the period before the final isolation, as long as an open inlet existed and if the initial marine period was not too salty. This could be called the pre-isolation stock. The question about how rapid the final trapping of the post-isolation stock occurred is hard to solve with any certainty, but it most likely happened slightly before the deposition of the Eggøya tephra; we note sudden shifts in magnetic susceptibility and the Br/Zn ratios (Fig. 8) as well as in the PC1 values (Fig. 12) just prior to the tephra fall-out. This would also indicate that the Maria Musch outlet was tectonically raised above sea level slightly before we see any signs of an eruption, which was also inferred by Larsen et al. (2021). In this context

it should be emphasized that the subaerial tephra is the only sign of the eruption in the terrestrial environment, although the eruption started as submarine volcanism, possibly triggering the uplift. Later, when Nordlaguna had become an isolated lake due to the tectonic related uplift, Eggøya had turned into a subaerial tephra-producing volcano, spreading its tephra on the island as well as into Nordlaguna. This transition, from submarine to subaerial volcanism, was possibly a rapid process, cf. Surtsey, from a few weeks to years, which is also indicated by the relative timing of the isolation of NL and the tephra fall-out (Figs. 8 and 12).

Declaration of competing interest

The authors declare that they have no known competing financial interests or personal relationships that could have appeared to influence the work reported in this paper.

Acknowledgement

We are very grateful for the financial support from The Research Council of Norway (Grant No. 244135/E10 to A. Lyså), Arctic Field Grant/Research Council of Norway (personal grant to A. Lyså) (RIS-ID-ES538785) and the logistical support and necessary permissions provided by the County Governor of Nordland and the Norwegian Defence Logistic Organisation (CYFOR, Jan Mayen). Screening for diatoms by Christof Pearce (Århus University, previously at Stockholm University) showed that the sediments are almost totally barren of diatoms, but we are very grateful for his attempts to find any! Fredrik Høgaas is thanked for the help with sediment coring and we appreciate how the personnel and staff at the Jan Mayen Station and Torgeir Madsen at CYFOR kindly supported us with their hospitality and transport in the field. Irene Lundquist helped with some of the graphics. We are also grateful for an insight-full review and that Stig Skreslet provided us with interesting information and his publications from Jan Mayen and Nordlaguna.

Appendix A. Supplementary data

Supplementary data to this article can be found online at <https://doi.org/10.1016/j.qsa.2022.100060>.

References

- Anda, E., Orheim, O., Mangerud, J., 1985. Late Holocene glacier variations and climate at Jan Mayen. *Polar Res* 3, 129–140. <https://doi.org/10.3402/polar.v3i2.6946>.
- Anderson, J., 1746. *Nachrichten von Island, Grönland und der Strasse Davis*. Hamburg.
- Bang, C., Skreslet, S., 1965. Hydrobiologisk studentekspedisjon till Jan Mayen sommeren 1963. *Norsk Polarinstitutt, Årbok* 1963, 265–267. Oslo 1965.
- Barr, S., 2003. *Jan. Mayen Norges Utpost I Vest, Øyas Historie Gjennom 1500 År*. Schibsted forlag, Oslo, p. 264.
- Bird, C.G., 1935. Arctic char in Jan Mayen Island. *Salmon and Trout Magazine* 6, 141–146.
- Björck, S., Dearing, J.A., Jonsson, A., 1982. Magnetic susceptibility of Late Weichselian deposits in southeastern Sweden. *Boreas* 11, 99–111.
- Bronk Ramsey, C., 2009. Bayesian analysis of radiocarbon dates. *Radiocarbon* 51 (1), 337–360.
- Caley, T., Malaizé, B., Zaragosi, S., Rossignol, L., Bourget, J., Eynaud, F., Martinez, P., Giraudeau, J., Charlier, K., Ellouz-Zimmerman, N., 2011. New Arabian Sea records help decipher orbital timing of Indo-Asian monsoon. *Earth Planetary Science Letters* 308, 433–444. <https://doi.org/10.1016/j.epsl.2011.06.019>.
- Christoffersen, M., 2018. *Sedimentation in Nordlaguna – a Closed Basin on Jan Mayen*. MSc thesis. University of Tromsø, The Arctic University of Norway, Tromsø, p. 111.
- Cromwell, G., Tauxe, L., Staudigel, H., Constable, C.G., Koppers, A.A.P., Pedersen, R.-B., 2013. In search of long-term hemispheric asymmetry in the geomagnetic field: results from high northern latitudes. *Geochemistry, Geophysics, Geosystems* 14, 3234–3249.
- Fitch, F., Grasty, R., Miller, J., 1965. Potassium-argon ages of rocks from Jan Mayen and an outline of its volcanic history. *Nature* 207, 1349–1351.
- Gabrielsen, G.W., Brekke, B., Alsos, I.G., Hansen, J.R., 1997. *Natur- og kulturmiljøet på Jan Mayen – med en vurdering av verneverdier, kunnskapsbehov og forvaltning*. Norsk Polarinstitutt Meddelelser Nr 144, 127. Oslo.
- Gjerlow, E., Höskuldsson, A., Pedersen, R.B., 2015. The 1732 Surtseyan eruption of Eggøya, Jan Mayen, North-Atlantic: deposits, distribution, chemistry and chronology. *Bulletin of Volcanology* 77, 14. <https://doi.org/10.1007/s00445-014-0895-6>.
- Gjerlow, E., 2019. *Holocene Volcanic Activity and Hazards of Jan Mayen, North-Atlantic*. PhD thesis. University of Bergen.
- Guevara, S.R., Rizzo, A., Daga, R., Williams, N., Villa, S., 2019. Bromine as indicator of lacustrine sedimentary organic matter in paleolimnological studies. *Quaternary Research* 92 (1), 257–291. <https://doi.org/10.1017/qua.2018.125>.
- Hudson, S.R., Gjelten, H.M., Isaksen, K., Kohler, J., 2019. An Assessment of MOSJ. Environmental Status for Atmospheric and Terrestrial Climate in Svalbard and Jan Mayen. Norwegian Polar Institute Report 050, p. 42.
- Imslund, P., 1978. *The Geology of the Volcanic Island Jan Mayen, Arctic Ocean*, vol. 78. Nordic Volcanological Institute, p. 74.
- Larsen, E., Lyså, A., Björck, S., Ganerød, M., Höskuldsson, A., van der Lelij, R., Tassis, G., 2022. Volcanic and surficial process constraints on the formation of a lake basin in Jan Mayen, Norway. *Quaternary Science Advances* (in press).
- Larsen, E., Lyså, A., Höskuldsson, A., Davidsen, J.G., Nadeau, M.J., Power, M., Tassis, G., Wastegård, S., 2021. A dated volcanotectonic deformation event in Jan Mayen causing landlocking of Arctic charr. *Journal of Quaternary Science* 36, 180–190. <https://doi.org/10.1002/jqs.3280>.
- Lyså, A., Larsen, E.A., Anjar, J., Akcar, N., Ganerød, M., Hiksodal, A., Van der Lelij, R., Vockenhuber, C., 2021. The last glaciation of the Arctic volcanic island Jan Mayen. *Boreas* 50, 6–28. <https://doi.org/10.1111/bor.12482>.
- Lyså, A., Larsen, E., Hiksodal, A., 2022. JAN MAYEN, Kvartærgeologisk Kart (Quaternary Geological Map) M 1:50 000. Norges Geologiske Undersøkelse.
- Mayer, L.M., Schick, L.L., Allison, M.A., Ruttenberg, K.C., Bentley, S.J., 2007. Marine vs. terrigenous matter in Louisiana coastal sediments: the uses of bromine:organic carbon ratios. *Marine Chemistry* 107, 244–254. <https://doi.org/10.1016/j.marchem.2007.07.007>.
- McHugh, C.M.G., Gurung, D., Giosan, L., Ryan, W.B.F., Mart, Y., Sancar, U., Burckle, L., Cagatay, M.N., 2008. The last reconnection of the Marmara Sea (Turkey) to the World Ocean: a paleoceanographic and paleoclimatic perspective. *Marine Geology* 255, 64–82. <https://doi.org/10.1016/j.margeo.2008.07.005>.
- Mjelde, R., Breivik, A.J., Raum, T., Mittelstaedt, E., Ito, G., Faleide, J.I., 2008. Magmatic and tectonic evolution of the north atlantic. *Journal of the Geological Society of London* 165, 31–42.
- Mosj, 2019. Homepage. <https://www.mosj.no/en/climate/ocean/sea-ice-extent-bare-nts-sea-frac-strait.html>.
- Polyak, L., Alley, R.B., Andrews, J.T., Brigham-Grette, J., Cronin, T.M., Darby, D.A., Dyke, A.S., Fitzpatrick, J.J., Funder, S., Holland, M., Jennings, A.E., Miller, G.H., O'Reagan, M., Savelle, J., Serreze, M., St John, K., White, J.W.C., Wolff, E., 2010. History of sea ice in the Arctic. *Quaternary Science Reviews* 29, 1757–1778.
- Reimer, P.J., Austin, W.E.N., Bard, E., Bayliss, A., Blackwell, P.G., Bronk Ramsey, C., Butzin, M., Cheng, H., Edwards, R.L., Friedrich, M., Grootes, P.M., Guilderson, T.P., Hajdas, I., Heaton, T.J., Hogg, A.C., Hughen, K.A., Kromer, B., Manning, S.W., Muscheler, R., Palmer, J.G., Pearson, C., van der Plicht, J., Reimer, R.W., Richards, D.A., Scott, E.M., Southon, J., Turney, C.S.M., Wacker, L., Adolphi, F., Büntgen, U., Capano, M., Fahrni, S.M., Fogtmann-Schulz, A., Friedrich, R., Köhler, P., Kudsk, S., Miyake, F., Olsen, J., Reinig, F., Sakamoto, M., Sookdeo, A., Talamo, S., 2020. The INTCAL20 Northern Hemisphere radiocarbon age calibration curve (0–55 cal BP). *Radiocarbon* 62 (4), 725–757.
- Rothwell, R.G., Croudace, I.W., 2015. Twenty years of XRF core scanning of marine sediments: what do geochemical proxies tell us? In: Croudace, I.W., Rothwell, R.G. (Eds.), *Micro-XRF Studies of Sediment Cores. Developments in Paleoenvironmental Research* 17. Springer, Netherlands. https://doi.org/10.1007/978-94-017-9849-5_2.
- Sjöström, J.K., Bindler, R., Cortizas, A.M., Björck, S., Hansson, S.V., Karlsson, A., Ellertson, D.T., Kylander, M.E., 2022. Late Holocene peat paleodust deposition in south-western Sweden - exploring geochemical properties, local mineral sources and regional aeolian activity. *Chemical Geology* 606. <https://doi.org/10.1016/j.chemgeo.2022.120881>.
- Skreslet, S., 1969. The ecosystem of the arctic Lake Nordlaguna, Jan Mayen Island. I. General features and hydrography. *Astarte* 2, 27–34.
- Skreslet, S., Foged, N., 1970. The ecosystem of arctic Lake Nordlaguna, Jan Mayen Island. II. Plankton and benthos. *Astarte* 3, 53–61.
- Skreslet, S., 1973. The ecosystem of the arctic Lake Nordlaguna, Jan Mayen Island III. Ecology of arctic char. *Salvelinus alpinus* (L.). *Astarte* 6, 42–54.
- Sylvester, A.G., 1975. History and surveillance of volcanic activity on Jan Mayen Island. *Bulletin of Volcanology* 39 (2), 1–23.
- Taboada, T., Cortizas, A.M., Garcia, C., Garcia-Rodeja, E., 2006. Particle-size fractionation of titanium and zirconium during weathering and pedogenesis of granitic rocks in NW Spain. *Geoderma* 131, 218–236.
- Weltje, G.J., Tjallingii, R., 2008. Calibration of XRF core scanners for quantitative geochemical logging of sediment cores: theory and application. *Earth and Planetary Science Letters* 274, 423–438.